Accepted Manuscript

A generic contact detection framework for cylindrical particles in discrete element modelling

Y.T. Feng, K. Han, D.R.J. Owen

PII: S0045-7825(16)30319-X
DOI: http://dx.doi.org/10.1016/j.cma.2016.11.001
Reference: CMA 11211

To appear in: *Comput. Methods Appl. Mech. Engrg.*

Received date : 5 May 2016
received in revised form 11 October 2016
accepted 2 November 2016

Please cite this article as: Y.T. Feng, et al., A generic contact detection framework for cylindrical particles in discrete element modelling, *Comput. Methods Appl. Mech. Engrg.* (2016), http://dx.doi.org/10.1016/j.cma.2016.11.001

A Generic Contact Detection Framework for Cylindrical Particles in Discrete Element Modelling

Y. T. Feng[1]*, K. Han[2], and D. R. J. Owen[1]
[1] Zienkiewicz Centre for Computational Engineering, Swansea University, UK
[2] CD-adapco, UK

Abstract

This paper aims to develop a generic framework for detecting contact between cylindrical particles in discrete element modelling based on a full exploitation of the axi-symmetrical property of cylinders. The main contributions include: 1) A four-parameter based local representative system is derived to describe the spatial relationship between two cylinders so that the 3D cylinder-cylinder intersection problem can be reduced to a series of 2D circle-ellipse intersections, which considerably simplifies the contact detection procedure. 2) A two-stage contact detection scheme is proposed in which no-overlap contact pairs are identified in the first overlap check stage, and then the actual overlap region is determined in the second resolution stage and represented by two schemes: the layered representation which is generic, and the edge representation which is numerically more efficient but less accurate. 3) The most significant contribution is the development of two theorems that establish a fundamental relationship between the contact point and contact normal of two contacting cylinders, offering a simple approach to determining the normal direction based on the contact point and vice versa. These theorems are valid not only for cylinders, but also for any axi-symmetrical shapes and their combinations. Some numerical issues are discussed. Numerical examples are presented to illustrate the capability and applicability of the proposed methodologies.

KEYWORDS: Discrete element method, Cylindrical particle, Axi-symmetry, Non-spherical shape, Contact detection, Contact normal, Contact point

1 Introduction

The discrete element method (DEM) [1] has been firmly established as one of the most effective computational techniques for modelling systems exhibiting discrete or particulate behaviour in many scientific and engineering applications, especially in porous media, soil and geo-mechanics, agricultural and chemical engineering, pharmaceutical and material processing, to name a few. The success lies in its ability to model individual particle behaviour in the system concerned by effectively detecting possible physical contact on their boundaries, followed by evaluating the corresponding contact forces based on a set of contact interaction laws. Most of discrete element simulations that have been conducted so far employ circular or spherical particles, and problems with non-spherical particles are typically modelled by bonding or clumping spherical particles together to represent real non-spherical particles. There has been an increasing interest, particularly in industrial applications, in using non-spherical particle shapes as primitive discrete elements. Since the 1980s, there has been a

*Corresponding author; e-mail: y.feng@swansea.ac.uk

continued effort to develop discrete element models for non-spherical primitive objects, such as ellipses [2, 3, 4], ellipsoids [6, 7], super-quadrics [5, 12], dilated shapes [8], polygons [9, 13] and polyhedra [10, 11, 13, 14]. However, there is still a lack of theoretically derived contact models for non-spherical shaped particles in general [15] and non-smooth particles with edges and sharp corners in particular. The contact interactions between these contacting objects are often proposed in an *ad-hoc* manner.

There is limited work reported on discrete element modelling of cylinders in the literature. In addition to the lack of theoretically sound contact theories for cylinders, surprisingly sophisticated contact scenarios between cylinders with regard to the geometric aspect imposes another numerical challenge to adopt the cylinder as a primitive particle shape in DEM. Recently, Kodam *et. al* [16, 18] proposed a discrete element modelling approach for cylinders in which contact configurations between two cylinders are classified into several categories and identified according to a set of contact criteria. The corresponding contact overlap, location and normal are determined on a case-by-case base. The approach was experimentally validated [17] and the model is compared more favourable to the bonded sphere model in terms of the physical behaviour of the tested cases.

Nevertheless, this classification based approach has several disadvantages: 1) The listed contact configurations may not be comprehensive. For instance, some possible contact configurations for cylinders with very small height/radius ratios may be missing; 2) Many different checks and criteria involved make the procedure error prone; 3) The computations of the contact overlap and contact normal for most of the identified cases are often of an *ad-hoc* nature. As will become apparent later, the inappropriate choice of a contact normal may introduce superficial energy into the system and cause numerical instability in simulations.

More notably, the axi-symmetrical property of cylinders is not utilised in their approach. By recognising and fully exploiting this important property of cylinders, Chittawadigi and Saha [19] proposed a more effective local coordinate representation system for two cylinders. This representation, which is derived based on dual number algebra [19] and commonly used in robotic systems, uses only four so-called Denavit-Hartenberg parameters to represent the relative relationship of two cylinders. It essentially reduces the complexity of the contact detection problem from intersections of 3D cylinders to those of line and rectangle, and circle and ellipse in 2D, hence leading to a much simplified and more efficient contact detection algorithm.

On the adoption of this particular representation, and a further exploitation of the axi-symmetrical property of cylinders, this paper develops a more generic and effective computational framework for undertaking contact detection between cylindrical particles in discrete element modelling. Particularly, a two-stage contact detection procedure is proposed in which no-overlap contact pairs are excluded in the first stage, and then the overlap region between a contacting cylindrical pair is determined and represented in the second stage by either the layered region or edge representation. This procedure imposes no limitations, at least theoretically, on (relative) sizes and aspect ratios of cylinders, and minimises the number of possible checks for different contact configurations, thereby resulting in a more generic and robust cylinder contact detection framework. The most significant contribution is the development of two theorems that establish a fundamental relationship between the contact point and contact normal for two contacting cylinders such that if one is specified then the other can be determined. More remarkably, these two theorems are valid not only for cylinders but also for any axi-symmetrical shapes and their combinations.

Note that the current work only deals with contact detection issues which are related to the geometric aspect of discrete element modelling of cylinders, while physically related issues,

such as contact interaction laws for cylinders, will not be addressed. Also both terms, *overlap* and *contact*, are interchangeable in most places.

The paper is organised as follows: In the next section, the four-parameter geometric representations for a two-cylinder system are derived in a simple and straightforward manner. Then the two-stage contact detection procedure is described in detail in Section 3. Determinations of the contact geometric features of an overlap region are discussed in Section 4, and more importantly, the two contact point and normal related theorems are presented. Some related numerical and implementation issues are discussed in Section 5. A number of numerical examples are provided in Section 6 to illustrate the capability and applicability of the method. The main features of the proposed methodology are summarised in Section 7. Some technical details are presented in Appendices.

2 Geometric Description and Coordinate Representation of A Two-Cylinder System

A cylinder is fully described by its two geometric features, radius r and half height h, and two spatial position properties, axial direction $\mathbf{n}$ (unit vector) and central coordinates $\mathbf{c}$, which is denoted as $\mathcal{C}:\{r, h, \mathbf{n}, \mathbf{c}\}$. Set up a local coordinate system $\{x, y, z\}$ with the origin at the centre and the z-axis along the cylinder axis defined by $\mathbf{n}$, as shown in Figure 1(a). The reflective symmetry of a cylinder about the local x-y plane means that $\mathbf{n}$ and $-\mathbf{n}$ can be equally chosen to define the z-direction; while the axi-symmetrical nature permits us to freely choose the most appropriate x- and y-axes for the problem concerned. It is this feature that will be fully exploited, leading to a set of coordinate systems for two cylinder contact detection described below.

Consider two cylinders denoted as $\mathcal{C}_i:\{r_i, h_i, \mathbf{n}_i, \mathbf{c}_i\}$ $(i = 1, 2)$, as shown in Figure 1(b). Define the angle between the two axes as α with

$$\cos\alpha = \mathbf{n}_1 \cdot \mathbf{n}_2 \tag{1}$$

It is required that $0 \leq \cos\alpha < 1$; otherwise if $\cos\alpha < 0$, simply set $\mathbf{n}_2 = -\mathbf{n}_2$. Thus $0 < \alpha \leq \pi/2$. Note that $\cos\alpha = 1$ or $\alpha = 0$, i.e. the two cylinders are in parallel, is a special case that will be considered in Section 4.

Let $\{X, Y, Z\}$ be the default global coordinate system for the problem concerned, and $\{x_i, y_i, z_i\}$, $(i = 1, 2)$ be the two local coordinate systems associated with the two cylinders with $\{\mathbf{e}_{x_i}, \mathbf{e}_{y_i}, \mathbf{e}_{z_i}\}, (i = 1, 2)$ as their corresponding unit vectors, in which the z_i axes are fixed to be $\mathbf{e}_{z_i} = \mathbf{n}_i$, but the x_i- and y_i-axes are to be determined.

First construct the shortest line segment between the two cylinder axes with the intersection points o_1 and o_2 on the two axes, as shown in Figure 1(b), and introduce an intermediate system $\{x, y, z\}$ with the origin at o_1 and $\{\mathbf{e}_x, \mathbf{e}_y, \mathbf{e}_z\}$ as the unit vectors of the axes as follows. Choose the z-axis along the z_1-axis, $\mathbf{e}_z = \mathbf{e}_1$, and the x-axis along the shortest line. As the line is perpendicular to both axes, $\mathbf{e}_x$ can be defined as

$$\mathbf{e}_x = \frac{\mathbf{e}_{z_2} \times \mathbf{e}_{z_1}}{||\mathbf{e}_{z_2} \times \mathbf{e}_{z_1}||} \tag{2}$$

Then the y-axis is formed by

$$\mathbf{e}_y = \mathbf{e}_z \times \mathbf{e}_x \tag{3}$$

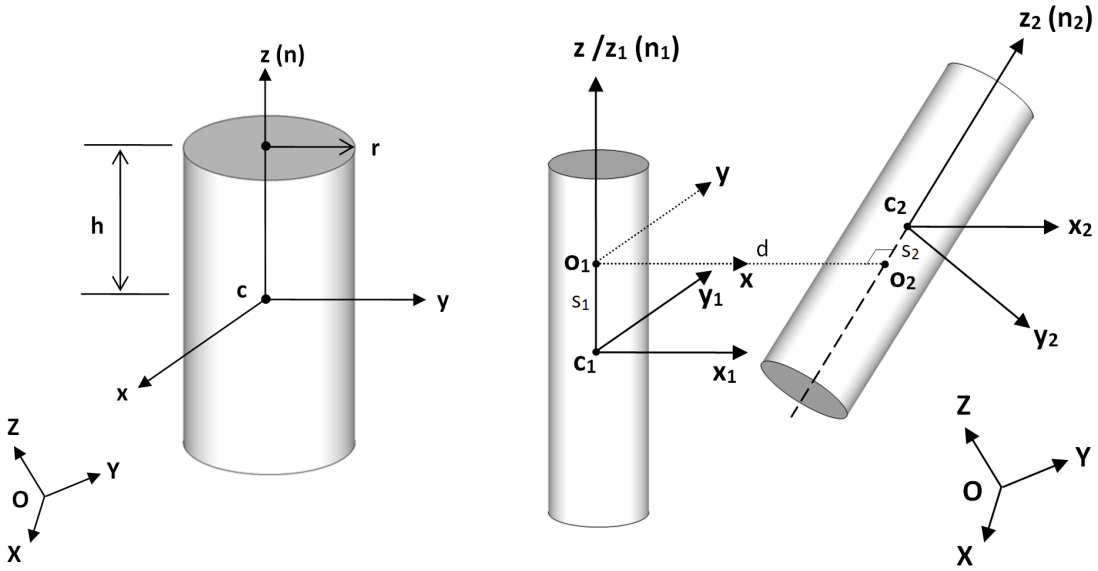

(a) One cylinder (b) Two cylinders

Figure 1: Global and local systems for (a) one cylinder; (b) two cylinders

Now the (signed) shortest distance between the two cylinder axes, $d = |o_1 o_2|$, can be calculated as

$$d = \mathbf{e}_x \cdot (\mathbf{c}_2 - \mathbf{c}_1) \tag{4}$$

For the two local cylinder systems, both x-axes are set to be along the same direction as the x-axis of the intermediate system:

$$\mathbf{e}_{x_i} = \mathbf{e}_x \quad (i = 1, 2) \tag{5}$$

and both y axes can be defined by

$$\mathbf{e}_{y_i} = \mathbf{e}_{z_i} \times \mathbf{e}_{x_i} \quad (i = 1, 2) \tag{6}$$

The (signed) distance between each cylinder centre to the intersection point of the cylinder axis with the shortest line segment, $s_i = |c_i o_i|\,(i = 1, 2)$, can be found:

$$s_1 = \frac{t_1 - t_2 \cos\alpha}{\sin^2\alpha}; \quad s_2 = -\frac{t_2 + t_1 \cos\alpha}{\sin^2\alpha} \tag{7}$$

where $t_i = \mathbf{e}_{z_i} \cdot (\mathbf{c}_2 - \mathbf{c}_1)$. Clearly, the first local system $\{x_1, y_1, z_1\}$ is a translation of the intermediate system $\{x, y, z\}$ along the z-axis:

$$x_1 = x; \quad y_1 = y; \quad z_1 = z + s_1 \tag{8}$$

while the second local system $\{x_2, y_2, z_2\}$ is first a translation of the intermediate system along the x-axis to o_2, followed by a rotation about the x-axis with an angle of α and then by another translation in the z-axis to the cylinder centre $\mathbf{c}_2$:

$$\begin{aligned} x_2 &= x + d \\ y_2 &= +\cos\alpha\, y + \sin\alpha\, z \\ z_2 &= -\cos\alpha\, y + \cos\alpha\, z + s_2 \end{aligned} \tag{9}$$

Now through the intermediate system, the coordinate transformation between the two local systems can be obtained as

$$\mathbf{x}_1 = \mathbf{c}_{12} + \mathbf{T}_{12}\mathbf{x}_2; \qquad \mathbf{x}_2 = \mathbf{c}_{21} + \mathbf{T}_{21}\mathbf{x}_2 \tag{10}$$

where $\mathbf{c}_{12}(\mathbf{c}_{21})$ are the coordinates of the centre $c_2(c_1)$ at the local system of cylinder $\mathcal{C}_1(\mathcal{C}_2)$:

$$\mathbf{c}_{12} = [+d, -s_2 \sin\alpha, s_1 - s_2 \cos\alpha]^T \tag{11}$$

$$\mathbf{c}_{21} = [-d, +s_1 \sin\alpha, s_2 - s_1 \cos\alpha]^T \tag{12}$$

and the transformation matrices $\mathbf{T}_{12}$ and $\mathbf{T}_{21}$ are

$$\mathbf{T}_{12} = \begin{bmatrix} 1 & 0 & 0 \\ 0 & +\cos\alpha & \sin\alpha \\ 0 & -\sin\alpha & \cos\alpha \end{bmatrix} = \mathbf{T}_{21}^T \tag{13}$$

The coordinate transformation from either of the two local systems to the global can be expressed as

$$\mathbf{X} = \mathbf{c}_i + [\ \mathbf{e}_{x_i}\ \ \mathbf{e}_{y_i}\ \ \mathbf{e}_{z_i}\ ]\,\mathbf{x}_i \quad (i = 1, 2) \tag{14}$$

where $\mathbf{x}_i$ is a local coordinate vector and $\mathbf{X}$ is the corresponding global coordinate vector. All vectors are assumed in columnwise format.

The above formulae provide a numerically efficient geometric system and fully describe the geometric relationship of two cylinders in both local and global coordinate systems. It is important to highlight that only four parameters, d, α, s_1 and s_2, are needed to fully represent the relative relationship of two cylinders, as first presented in [19].

Also note that the above systems are established on the basis that $\mathcal{C}_1$ is the leading or master cylinder, while it may be necessary to temporarily choose $\mathcal{C}_2$ to be the leading cylinder instead for certain contact scenarios inside the $\mathcal{C}_1$-$\mathcal{C}_2$ contact pair, as will be discussed later. This can readily be achieved in the local systems by just setting $\alpha = -\alpha$, and swapping s_1 and s_2, r_1 and r_2 and h_1 and h_2, while anything else remains the same. In addition, when any local vector needs to be transformed to the global system, both x and y components should be multiplied by -1.

The key to the proposed geometric description system is the choice of both local x-directions to be the same as that of the common shortest line $\mathbf{e}_{x_1} = \mathbf{e}_{x_2} = \mathbf{e}_x$. This implies that the two local x coordinates only differ by the shortest distance d:

$$x_1 = x_2 + d \tag{15}$$

The most important consequence is, however, that both cylinders become rectangles when they are projected on the y-z plane of any of their local coordinate systems, and are parallel on both x-z and x-y planes, as illustrated in Figure 2. These features significantly facilitate the contact detection for two cylinders by decoupling a 3D geometric problem into a few much simpler and well-defined 2D problems, as will be demonstrated in the following section. Also note that the proposed geometric description system is developed purely based on the axi-symmetrical property of cylinders and therefore can be extended to describe the relative spatial relationship between any pair of axi-symmetrical objects.

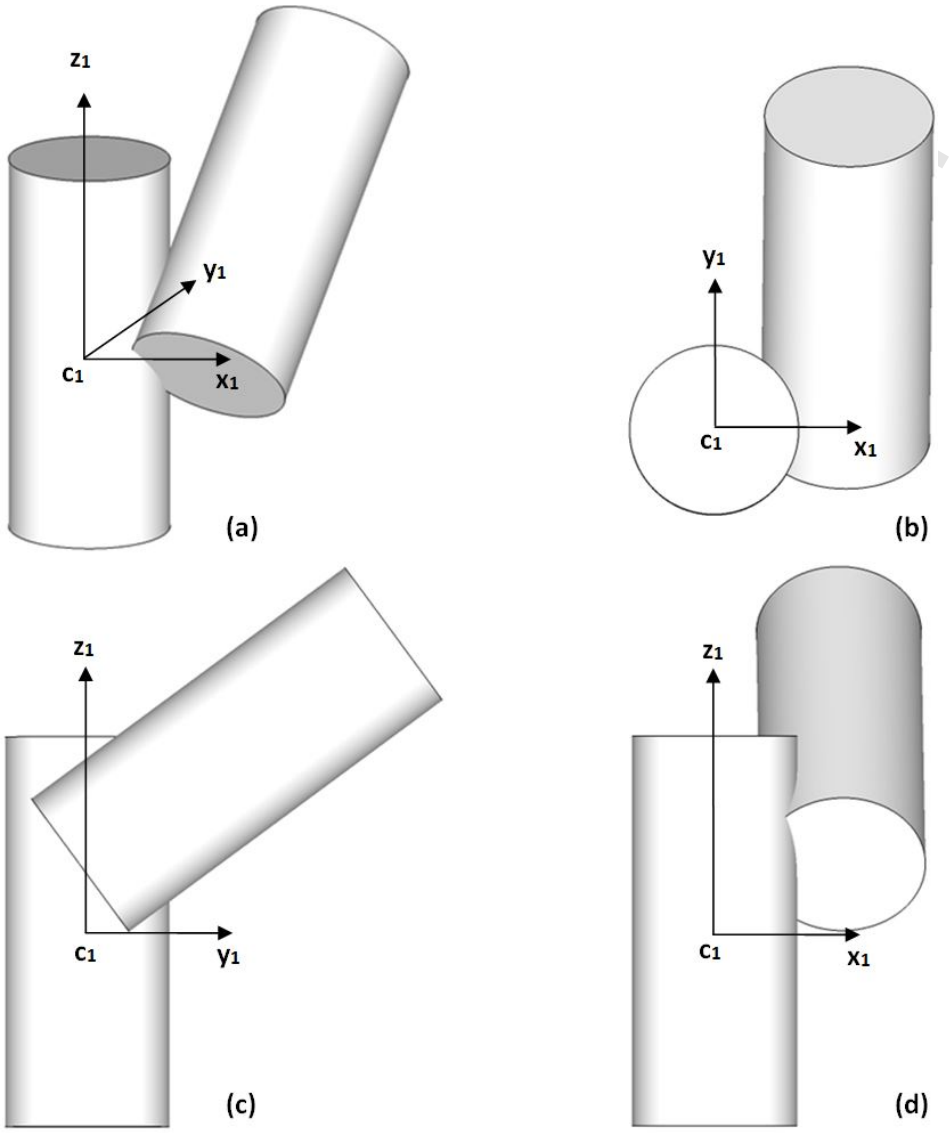

Figure 2: Two intersecting cylinders (a) and their projects on the x_1-y_1 plane (b); the y_1-z_1 plane (c); and the x_1-z_1 plane

3 Contact Detection of Two Cylinders

This section describes a procedure to check if there exists an overlap between a given pair of cylinders $\mathcal{C}_1$ and $\mathcal{C}_2$. The next section discusses how to obtain some overlap features when such a contact is established. As the overlap check is conducted locally, the local coordinate system of $\mathcal{C}_1$, $\{x_1, y_1, z_1\}$, can be considered as the global system. This not only simplifies the following description and discussion, but also gives rise to more efficient numerical procedures. By utilising the fact that now $\mathbf{e}_{x_1} = [1,0,0]^T, \mathbf{e}_{y_1} = [0,1,0]^T, \mathbf{e}_{z_1} = [0,0,1]^T$ and $\mathbf{c}_1 = [0,0,0]^T$, some operations involving these vectors may be much simplified. Only when some local vectors, such as a contact normal, need to be transformed to the global system afterwards, the actual local-global transformation (14) needs to be performed.

The current work proposes a two-stage contact detection procedure. The first stage performs a series of relatively computationally inexpensive checks in order to exclude no-contact cases

at an early stage, and thus is termed the *non-overlap check* stage. When a possible contact cannot be excluded, further verification and checks will be performed in the second *overlap resolution* stage where some contact overlap properties, such as overlap (penetration), contact point, and contact normal etc, are also be evaluated if an actual overlap does exist.

3.1 Non-Overlap Checks

An effective contact detection procedure should be able to identify no-contact cases as early as possible and with minimum computational costs. The proposed non-overlap check procedure sequentially involves up to three steps, with increased computational complexity, to establish if an overlap exists for the given cylinder pair. As soon as a no-contact case is identified at the current step, the procedure terminates; Otherwise, the next step is executed.

Step 1: Interior contact check. The shortest distance d between the two cylinder axes is checked first. If

$$|d| \geq r_1 + r_2 \tag{16}$$

then there is no contact, and the procedure stops; Otherwise check if the two intersection points between the shortest line with the two cylinder axes, o_1 and o_2, are located within both cylinders:

$$|s_1| < h_1 \text{ and } |s_2| < h_2 \tag{17}$$

If so, an actual contact is established and the procedure stops. This is the simplest contact scenario, termed the *interior contact*. When the two conditions (17) are not all satisfied, move to the next step for a further check.

Step 2: Profile overlap check. The second step performs an overlap check on the projections of the cylinders on the y_1-z_1 plane of $\mathcal{C}_1$ which are two rectangles as shown in Figure 2(c). Obviously, the two cylinders are not in contact if the two rectangles have no overlap. First check if the bounding box of the rectangle of $\mathcal{C}_2$ is in overlap with the first rectangle. Otherwise, apply, e.g. the classic Cohen-Sutherland Line Clip algorithm [20] or similar methods to further establish if the two rectangles are in overlap.

Step 3: Minimum distance check.

Up to this step, an interior contact case has been ruled out, i.e. at least one of the two intersection points of the shortest line with the two cylinder axes, o_1 and o_2, must be located outside one of the cylinders. It can be concluded, therefore, that if the two cylinders are in contact, at least one of the four base disks penetrates into the other cylinder with the maximum penetration, or equivalently, that the minimum distance from the edge of at least one base disk to the axis of the other cylinder must be smaller than the radius of that cylinder. It is, however, not obvious in general which base disk of which cylinder will have the minimum distance. Therefore, this step may check up to two base disks, one from each cylinder and against the other cylinder to evaluate the corresponding minimum distance. By default, the check starts from one of the base disks of $\mathcal{C}_2$ against $\mathcal{C}_1$ on the x_1-y_1 plane, and then swap $\mathcal{C}_1$ and $\mathcal{C}_2$ and repeat the procedure.

Refer to Figure 2(b) where the projection of $\mathcal{C}_1$ is a circle of radius r_1, while the projection of $\mathcal{C}_2$ is a tablet-shaped area, parallel to the y_1-axis. The $\mathcal{C}_2$ projection can lie in any of the four quadrants in the x_1-y_1 system. When the projected cylinder axis lies across two quadrants, the two base disks will not have the minimum distance. In this case $\mathcal{C}_1$ and $\mathcal{C}_2$ should be swapped and the check should be conducted for the two base disks of $\mathcal{C}_1$ against $\mathcal{C}_2$. Thus, without loss of generality, it is assumed that the entire projected cylinder axis of $\mathcal{C}_2$ is located in the first quadrant. By comparing the y_1 coordinates of the centres of the two base disks,

the one with a smaller coordinate should have the minimum distance, and thus should be used in the calculation.

The projection of the base disk, and indeed any cross-section disk of $\mathcal{C}_2$ is an ellipse of major radius $a = r_2$ and minor radius $b = r_2 \cos\alpha$, with the major axis parallel to the x_1 direction. The projected point of the base centre of $\mathcal{C}_2$ has the coordinates $(x_0, y_0) = (d, s_2 \sin\alpha)$. The minimum distance of the base to the axis of $\mathcal{C}_1$ is the minimum distance of the ellipse edge to the origin of the x_1-y_1 system, or mathematically it can be stated as the following minimum value problem:

$$d_{min} = \min_{x,y}\{x^2 + y^2\},\ \text{s. t. } \frac{(x - x_0)^2}{a^2} + \frac{(y - y_0)^2}{b^2} = 1 \tag{18}$$

This problem can be solved iteratively using the Newton-Raphson method, or be formulated as a quartic equation. The detail can be found in Appendix 1. When the obtained minimum distance $d_{min} \geq r_1$, it can be concluded that there is no contact between the two cylinders. Otherwise, swap $\mathcal{C}_1$ and $\mathcal{C}_2$, and repeat the above procedure. When the two checks both return a minimum distance smaller than the radius, there is still a possibility that the two cylinders may not be in contact. Such a case may occur when the closest point obtained on the ellipse lies outside the other cylinder. This is because the master cylinder is implicitly assumed infinitely long, and no consideration is given to a possible overlap between the base disks of the two cylinders, as this would involve more computations which is undesirable at this stage. These missed no-overlap situations can be resolved in the next resolution stage.

From the overlap check perspective, the about minimum problem is equivalent to an overlap check between the ellipse of the base disk of $\mathcal{C}_2$ and the cross-section circle of $\mathcal{C}_1$. Again, this can be formulated as the solution of a quartic equation (see Appendix 1). A no-contact situation arises when there is only one or no solution to the equation. The solution procedure to find the roots of the equation will be discussed later.

3.2 Overlap Region Resolution

The previous stage has identified and excluded almost all no-overlap cases. The main purpose of this stage is to further describe the intersection or overlap region of the two cylinders concerned, and in particular, to extract some of the geometric characteristics required for the contact force calculations in the subsequent physical modelling phase in DEM. In the process, some overlooked no-overlap cases in the previous stage will be identified.

The overlap region can exhibit many different complex shapes, depending on the shapes and relative configurations of the two cylinders, which hampers any attempt to accurately represent its geometric features. Some of the possible overlap cases are depicted in Figure 3. Nevertheless, the overlap region is convex and can be viewed as the intersection of the same two cylinders which are infinitely long, but truncated by at least one and at most four bases, i.e the region is always formed by the two side surfaces together with one to four base planes. The irregularity and complexity of the region increase when more bases are involved and particularly when some of them also intersect. Under the small overlap assumption made in the DEM, the overlap region can be small in the three directions, or small in two directions but large in the third direction, or small in one direction but large in the other two.

The geometric features of the overlap region to be extracted depend on the requirement of the contact physical model used for cylinders. As mentioned in the introduction, currently there are no specific physical contact models for cylinders, and various linear or nonlinear spring models are commonly used instead. For this type of models, the required contact

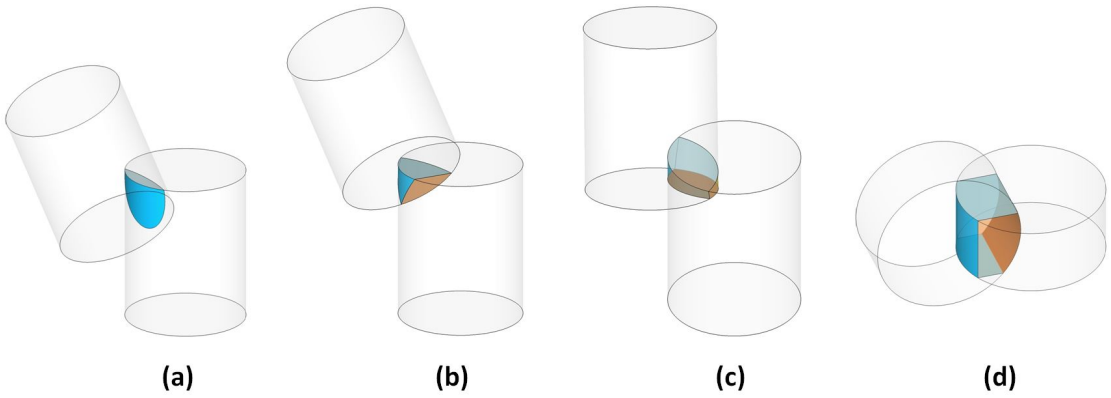

Figure 3: Some overlap regions, each involving two sides plus one, two or four base disks

geometric features include the (maximum) overlap, contact point and contact normal. For other models, such as the energy based models [9, 13], the contact width, area and/or volume may be required. To accommodate all possible contact models, the current work attempts to develop two overlap region representation schemes, from which the required geometric features can be evaluated.

3.3 Layered Overlap Region Representation

Define $\mathcal{R}$ to be the overlap region of the two cylinders $\mathcal{C}_1$ and $\mathcal{C}_2$: $\mathcal{R} = \mathcal{C}_1 \cap \mathcal{C}_2$. One of its faces must be the intersection of one base disk of one cylinder with the other cylinder. Without loss of generality, assume that this disk is the top base of $\mathcal{C}_1$. At a position $|z_1| < h$, the cross-section of $\mathcal{C}_1$ is a circular disk of radius r_1, denoted as $D(z_1)$. Then the cross-section of $\mathcal{R}$ at z_1 is the intersection of $D(z_1)$ with $\mathcal{C}_2$, denoted as $\mathcal{A}(z_1) = D(z_1) \cap \mathcal{C}_2$. Thus

$$\mathcal{R} = \{\mathcal{A}(z_1), h_0 < z_1 \leq h\} \tag{19}$$

where h_0 is the lower bound of z_1 at which $\mathcal{A}(z_0) = \varnothing$. This definition offers a parameterisation or layered representation of the overlap region, provided that each cross-section area $\mathcal{A}$ can be described. In the actual implementation, z_1 has to be discretised, leading to a discretised layer representation.

The key operation of this representation scheme is therefore to determine the cross-section area $\mathcal{A}(z_1)$. Depending on z_1, the cross-section of $\mathcal{C}_2$ can be a complete or truncated ellipse at one or possible two ends if one or two of its bases are also cut through by the plane at z_1. Figure 3 shows the cross-sections of $\mathcal{C}_1$ and $\mathcal{C}_2$ at the position $z_1 = h_1$ projected on the x_1-$y_1$plane, while the horizontal line represents the cross-line of the bottom base disk. The overlap area $\mathcal{A}$ (the shaded area in Figure 4(b)) is bounded by the circular and elliptical arcs (maybe more than one arc for each type) and up to the two line segments. The major and minor radii of the ellipse are $a = r_2/\cos\alpha$ and $b = r_2$, with the major axis parallel to the y_1, and the central coordinates being

$$(x_0, y_0) = (d, s_2 \sin\alpha) \tag{20}$$

To determine the boundary segments of $\mathcal{A}$, the intersection points of the disk and the ellipse need to be found. Mathematically this is again equivalent to solving a quartic equation. The detail can be found in Appendix 2. The number of solutions can be 0, 2 or 4. However,

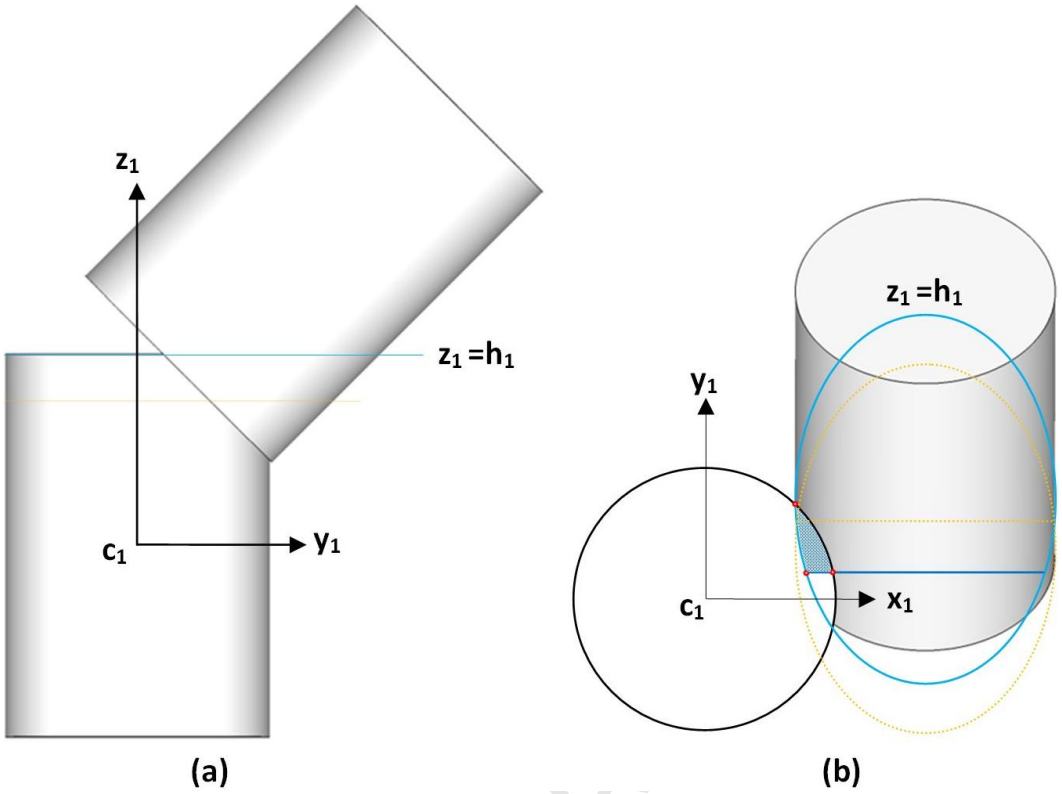

Figure 4: Projections of two intersecting cylinders and two cuts on the y_1-z_1 plane (a) and the x_1-y_1 plane (b).

the no-solution case does not necessarily mean that there is no overlap between the circle and the ellipse because one may be entirely enclosed by the other. Then the intersections between the circle/ellipse and the two base disk lines, if present, can be readily obtained. By processing these intersection points, an ordered boundary segment representation of $\mathcal{A}$ can be obtained. It is convenient to use the parametric form to represent each circular or elliptical arc involved. Furthermore, the arcs can be discretised, resulting in a more general polygon representation of the overlap area $\mathcal{A}$.

With the above boundary representation scheme, the geometric features of $\mathcal{A}$, such as the centroid and area, can be evaluated and queried. When all $\mathcal{A}(z_{1_i})$ are processed and represented, the whole overlap region $\mathcal{R}$ is described in a stack of (polygonal) layers, and its typical geometric features can be calculated.

This layer representation scheme offers a generic framework to represent the overlap region between two cylinders and can also be extended to more general cases, such as two axisymmetrical shaped objects. Both accuracy and numerical efficiency of the representation depend on the number of layers used. A higher accuracy can be achieved with more layers, but with higher computational costs.

The use of this scheme for large scale DEM problems, however, may be very limited, as the computational costs involved may be substantial even with a small number of layers. In the DEM, physical and numerical errors introduced in various stages of the modelling can be far greater than that of using a crude approximation for the overlap region. Thus an alternative representation scheme for the overlap region is proposed.

3.4 Edge Representation of Overlap Region

This alternative scheme attempts to represent all the edges in $\mathcal{R}$ that are associated with the bases, but ignore those formed by the two side surfaces of the cylinders. Each such edge can be constructed and represented as the intersecting boundary between a base disk and the other cylinder following the procedure outlined in the previous subsection. Although up to four bases can be involved in the formation of $\mathcal{R}$, it suffices that at most two bases are needed. These two bases should be considered from the same cylinder if they are both in actual overlap with the other cylinder; Otherwise one base from each cylinder is used. When only one base is involved in the overlap region, i.e. the so-call *edge-side* overlap scenario (see Figure 3(a)), the peak or lowest point of the region should be located and added as an extra point (or a degenerated edge) to represent the overlap region.

When all the intended edges are found, $\mathcal{R}$ is approximated as the convex hull formed by these edges. This edge representation provides a reasonable approximation to the actual region and can capture its main geometric features. Because the maximum number of the base-cylinder intersection operations is two, this representation scheme is much more computationally effective than the previous layered representation.

In the above two representation schemes, the cases that need to be checked individually are the intersections between the base disks and the other cylinder, thus clearly defined and the number of checks minimised. Also no restrictions are imposed on the cylinders in terms of their (relative) sizes and height/diameter ratios. Therefore, the proposed contact detection procedure provides a generic and unified computational framework for cylinders regardless of their size, shape, position and orientation.

4 Contact Geometric Features

When the overlap region has been represented, the following contact geometric features associated with the region will be considered: the overlap or (maximum) penetration, overlap area, overlap volume, contact point and contact normal. These may be sufficient for most of the physical contact models currently employed in the DEM. It is worth mentioning that, except for the contact volume, the other quantities are not well defined in general and are often evaluated in an *ad-hoc* manner. This is due to a lack of a general contact theory for irregularly shaped particles in the DEM.

4.1 Overlap, contact area and contact volume

The contact or overlap volume of $\mathcal{R}$ can be calculated from either the layered or edge representation, so no further discussion is needed.

The overlap is often defined as the maximum penetration of one object into another. This may be valid for sphere and other smoothly shaped objects, such as ellipsoids, but may not be the case for irregularly shaped objects in general. In fact, representing the maximum penetration as the overlap may be valid when the normal contact direction is more or less well-defined. In other words, the overlap may also be related to the choice of the normal direction. Nevertheless, even when the contact normal is defined, the overlap may not be taken as the maximum dimension of the overlap region in this direction. It may often be incorrect to define the overlap as the maximum penetration of $\mathcal{R}$, or the maximum distance between the two cylinder surfaces.

Let $\Delta x, \Delta y$ and Δz be the bounding box dimensions of the overlap region in the current coordinate system, which could be viewed as the maximum penetrations along the three directions. In theory, it may be better to find one direction along which the maximum penetration is the smallest. This, however, is difficult to achieve in a computationally efficient manner, and thus may not be practical. It is proposed that the overall overlap of $\mathcal{R}$ be defined as

$$\delta = \lambda / \sqrt{\frac{1}{\Delta^2 x} + \frac{1}{\Delta^2 y} + \frac{1}{\Delta^2 z}} \tag{21}$$

where the constant factor $\lambda = 2$ is introduced to modify the overall overlap. It is because if $\lambda = 1$, δ is appropriate when one of the three overlap dimensions is much smaller, but may be too small when all the three dimensions are comparable. However, in some situations the overlap in one particular direction may be smaller than those in the other perpendicular directions. For instance, in a *side-by-side* contact, the overlap of the two cylinders in the radial direction (of $\mathcal{C}_1$ for instance), Δr, may be smaller than Δz. In this case, the overall overlap may be more appropriately defined as

$$\delta = \lambda / \sqrt{\frac{1}{\Delta^2 r} + \frac{1}{\Delta^2 z}} \tag{22}$$

It is noted that without a rigorous definition that is compatible with the physical contact model used, the overlap may be subject to discontinuous change during a dynamic contact condition, causing artificial numerical errors or even numerical instability.

4.2 Contact point and contact normal

The contact point specifies the point at which the contact forces exert on the two objects in contact, while the contact normal specifies the unit direction of the normal forces. In what follows, the contact normal can also be used to represent the actual normal contact line which passes through the contact point.

The normal contact line is uniquely determined only for the interior contact case, which is coincided with the local x-axis described by (2) and (7). The contact point can be chosen at a point along the contact line within the contact region. For other contact cases, as discussed in the previous section, how to determine their contact points and normal contact lines are much less clear.

There are several options for the contact point: at the centroid of the region, on the surface of one cylinder, or at some other places within the overlap region. There is no much difference between these three options when all the three overlap dimensions are comparable, but the difference can be significant if the overlap along at least one direction is much larger than the rest. One example is the (near) *base-base* contact scenario (Figure 3(c)), where the overlap area is comparable with the cross-sections of the cylinders. In this case, using the centroid of the region is a better choice.

On the other hand, contact normal directions are not well defined for most general contact scenarios involving non-spherical, especially non-smooth objects including cylinders, due to a lack of a theoretically sound general contact theory for these particles in the DEM. In the previous work on cylinder contact [16], the normal contact direction is specified on a case-by-case basis, but is essentially in an *ad-hoc* fashion.

The present work proposes a novel approach to determine the contact normal if the contact point is given, based on the following statement:

Normal Contact Statement. *The contact normal starting from the contact point must pass through the two cylinder axes at the same time.*

This statement can be validated by a simple physical reasoning as follows. Considering two cylinders, which are fully fixed except for the freely rotational movement about their individual axes, that are brought in contact with a known contact point. Then a pair of normal forces will be exerted at the contact point of the two objects along the (opposite) normal direction. If the normal direction does not intersect with the two axes, at least one normal force will produce a non-zero moment about a cylinder axis and thus accelerate the rotation of that cylinder. As the overlap region and other contact quantities do not change with the rotation of the cylinder(s), an increasing amount of external energy from the force(s) will be continuously injected into the system, inevitably causing a system crash. Therefore, the normal contact forces and hence the contact normal have to pass through the two cylinder axes.

The next important question is: can such a normal direction be found? The following so-called **contact normal theorem** provides the answer.

Theorem 1 (Contact Normal Theorem)**.** *For a given pair of cylinders,* $\mathcal{C}_i$:$\{r_i, h_i, \mathbf{n}_i, \mathbf{c}_i\}$ $(i = 1, 2)$*, that are in contact with contact point at* $\mathbf{p}$*, if* $\mathbf{n}_1$*,* $\mathbf{n}_2$ *and* $\mathbf{p}$ *are not co-planar, the corresponding contact normal* $\mathbf{n}$ *from* $\mathcal{C}_1$ *to* $\mathcal{C}_2$ *can be uniquely determined by:*

$$\mathbf{n} = (\mathbf{p} - \mathbf{c}_1) - \frac{(\mathbf{p} - \mathbf{c}_1) \cdot \mathbf{n}_{p_1}}{\mathbf{n}_2 \cdot \mathbf{n}_{p_1}} \mathbf{n}_1 = (\mathbf{c}_2 - \mathbf{p}) - \frac{(\mathbf{c}_2 - \mathbf{p}) \cdot \mathbf{n}_p}{\mathbf{n}_2 \cdot \mathbf{n}_p} \mathbf{n}_2; \tag{23}$$

$$\textit{with} \quad \mathbf{n}_{p_i} = \mathbf{n}_i \times (\mathbf{c}_i - \mathbf{p}) \quad (i = 1, 2)$$

The proof of the above theorem is presented in Appendix 3. For the exceptional case where both cylinder axes and the contact point are co-planar, which includes the two cylinders in parallel as a special case, the contact normal will be on the same plane, and thus passes through the two axes, but cannot be determined by (23). In this case, the problem is reduced to a 2D rectangle-rectangle contact problem from which the contact normal may be obtained based on additional principles, for instance, the energy model for polygons [9, 13]. A non-solution case only occurs when the two axes are on the same plane, thus intersecting with each other, while the contact point is not co-planar. In this case, it is the contact point that is in a wrong position.

In the development of the above theorem, the other geometric features, except for axi-symmetry, of a cylinder play no part. Therefore the following broader and powerful conclusion can be drawn:

Corollary 1.1 (Corollary of Contact Normal Theorem)**.** *The contact normal theorem is valid for all axi-symmetrical geometric entities and their combinations.*

The theorem also implies that the same contact normal can be shared by different contact points as long as they are co-linear with the contact normal. In fact we have the following **contact point theorem**, or the converse of the contact normal theorem, to confirm this implication.

Theorem 2 (Contact Point Theorem)**.** *For a given pair of cylinders,* $\mathcal{C}_i : \{r_i, h_i, \mathbf{n}_i, \mathbf{c}_i\} (i = 1, 2)$*, that are in contact with a known contact normal direction* $\mathbf{n}$*, the contact point* $\mathbf{p}$ *should satisfy the following condition:*

$$\mathbf{p} = \mathbf{c}_i + t_i \, \mathbf{n}_i + \lambda \, \mathbf{n} \tag{24}$$

where

$$t_i = \frac{\mathbf{n} \cdot [(\mathbf{c}_1 - \mathbf{c}_2) \times \mathbf{n}_i]}{\mathbf{n} \cdot (\mathbf{n}_2 \times \mathbf{n}_1)} \quad (i = 1, 2)$$

and λ is an arbitrary constant.

The proof is given in Appendix 3. The presence of the free parameter λ in the above expression means that there are an infinite number of points on the normal contact line that can be chosen as the contact point. However, a proper contact point can be specified within or on the surface of the overlap region.

Both theorems reveal a fundamental relationship between the contact point and the contact normal, and offer a simple approach to determine the normal direction based on the contact point and vice versa. More significantly, the theorems can be applied to any axi-symmetrical objects in contact. They are of both theoretical and practical significance in that they not only remove the ambiguity in determining the normal direction and/or provide a means to fine tune the contact point, but also guarantee that no superficial rotational energy is introduced into the system, making the numerical simulation more stable. It is emphasised that the axi-symmetrical property plays a central role in the development of these theorems.

5 Other Issues

In the proposed contact detection framework, there are several numerical and implementation issues need to be addressed further.

5.1 Numerical Issues

The key numerical operation involved in the above proposed methodology is to find the intersection between a circle and an ellipse, i.e. solutions to a quartic equation. As every quartic equation is solvable by radicals, the roots of a quartic equation can be found analytically with a limited number of arithmetic operations. However, although this approach works well for most cases, it may not offer the best numerical efficiency and may fail for certain special cases. To this end, an iterative based numerical solution procedure is proposed as an alternative or complementary method in the present work.

The main part of this iterative approach lies in the use of Lin-Bairstow's method [21] to find the quadratic factors of a polynomial of any order. Let $P_n(x) = \sum_0^n a_i x^i$ be a polynomial of order n and choose two arbitrary parameters u and v, so that $P_n(x)$ can be expressed as

$$P_n(x) = (x^2 + ux + v)Q_{n-2}(x) + (cx + d) \tag{25}$$

where $Q_{n-2}(x)$ is a polynomial of order $n - 2$, and $cx + d$ is a remainder. The quadratic $x^2 + ux + v$ will be a quadratic factor of $P_n(x)$ when both c and d are zero, and thus its two roots are also the roots of the polynomial being solved. The Lin-Bairstow method uses Newton's method to adjust the coefficients u and v so that both c and d, which are a function of u and v, tend to zero. Next the polynomial is divided by the quadratic to reduce its order by 2. This process is iterated until the polynomial becomes a quadratic or a linear, and then all the roots can be determined.

Appendix 4 presents the Lin-Bairstow method for quartic equations. The method performs well for most cases with a typical number of iterations being 3 to 4 for a convergence tolerance of order 10^{-12}. When the solutions are found, they are also used as the initial guesses to

undertake a few local Newton iterations to improve their accuracy. This improvement step is important when the Lin-Bairstow method does not converge to the required accuracy in some rare cases. When only one solution is found, the quartic polynomial is deflated by the root to become a cubic equation which is either solved by an analytic approach or by the Lin-Bairstow method.

5.2 Implementation Issues

Although a general contact detection framework has been proposed which theoretically has the advantage of providing a universal procedure to conduct the contact detection for any cylinder contact situation, some special cases have to be treated separately in the implementation. For instance, when two cylinders are perpendicular to each other (i.e. $\cos\alpha = 0$), or when they are parallel, the general procedure will encounter some numerical difficulties, and thus these cases have to be treated specially. Also, when determining the contact overlap and point, different formulations may need to be adopted according to different contact scenarios, as mentioned in the previous subsection.

Owing to the finite precision nature of numerical operations, it is inevitable that tolerances have to be introduced in various stages of the contact detection procedure to distinguish different special contact cases and to control the convergence of the Newton method and Lin-Bairstow's method. However different selections of tolerance levels may lead to different simulation results, or cause more serious robustness issues.

5.3 Cylinder to Half-Space and Cylinder to Sphere Contact Detection

Other contact scenarios involving cylinders may be encountered in discrete element simulations, such as cylinder to half-space and cylinder to sphere. These two special contact cases can be simply handled within the current contact detection framework for two cylinders. By recognising the fact that both a half-space and a sphere can be viewed as the two special axi-symmetric geometric entities, the local coordinate systems similar to the one established in Section 2 can be obtained for these two contact cases. Under these systems, both cylinder to half-space and cylinder to sphere contact cases are reduced to 2D contact situations where the half-space is reduced to a straight line, the sphere to a circular disk, and the cylinder to a rectangle.

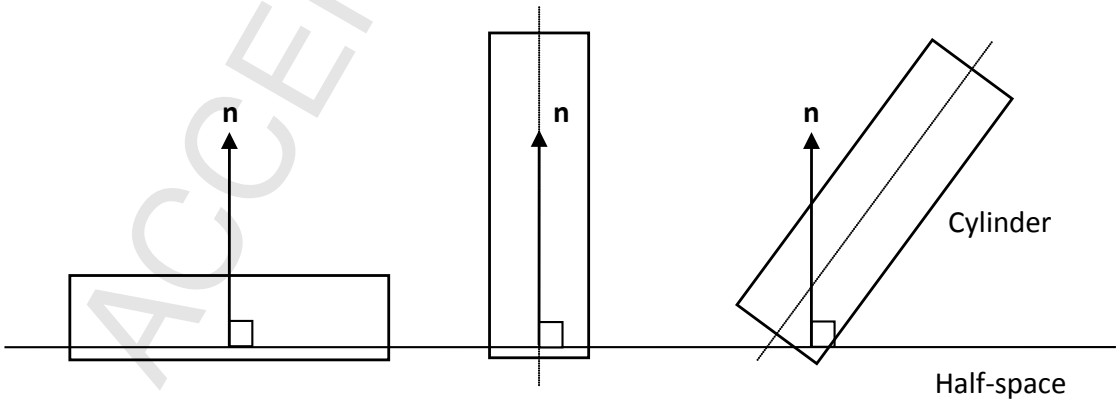

Figure 5: Three possible contact cases between a cylinder and a half-space: parallel, perpendicular and oblique

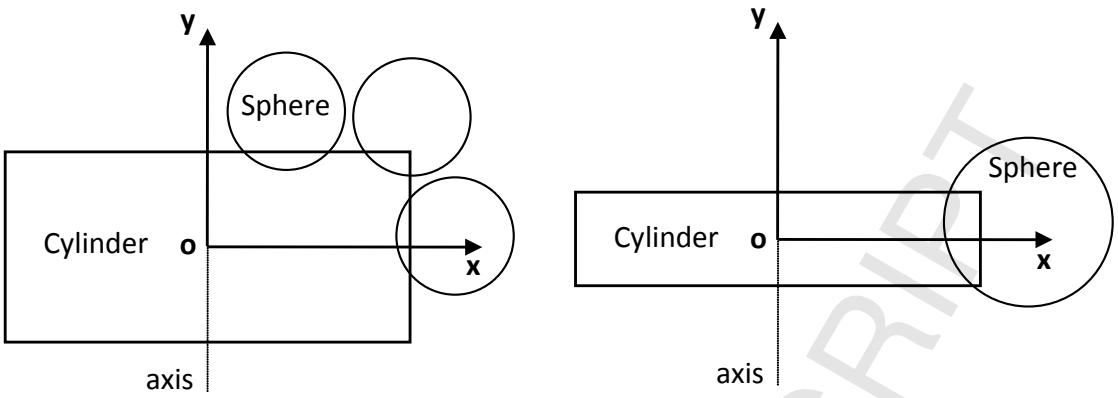

Figure 6: Four possible contact cases between a cylinder and a sphere

For the cylinder-half-space contact, there are three sub-cases to be considered, as shown in Figure 5: 1) the cylinder parallel to the plane; 2) the cylinder perpendicular to the plane; and 3) the cylinder in oblique contact with the plane. In all these cases, the normal of the plane is the contact normal, and the other contact features, such as overlap and contact point, may be readily defined.

For the cylinder-sphere contact, the cylinder centre is chosen to be the origin of the local x-y system. The cylinder axis will be the local y-axis but the positive direction is determined as such that the sphere centre is always on the first quadrant of the system. Then there are four sub-cases to be considered, as shown in Figure 6: 1) the sphere in contact with the top surface of the cylinder; 2) the sphere in contact with the side surface of the cylinder; 3) the sphere in contact with the top-right corner of the cylinder; and 4) the sphere in contact with the two corners or the whole side surface of the cylinder. The first two cases are trivial, while the third and fourth cases involve a corner contact which can be dealt with following the contact model proposed for polygons in [9], where both contact point and contact normal can be uniquely determined.

6 Numerical Examples

The above proposed contact detection methodology has been implemented in a commercial software STAR-CCM+ v11.02 [24] developed by CD-adapco, a global provider of multidisciplinary engineering simulation and design exploration software. The following numerical examples involving the simulation of the initial packing of cylinders are presented to illustrate the performance of the approach. Unlike circular disks and spheres, where some geometrically based packing algorithms [9, 23] have been developed to produce a reasonably dense initial packing, it is difficult to do so for cylinders. A typical approach for generating an initial packing for arbitrarily shaped particles is to inject particles into the packing region, and settle the particles with gravity and damping.

The current packing problem consists of randomly injecting cylinders with non-zero velocity into a cylindrical region. Under the action of the gravitational force and damping, the cylindrical particles will be settled to form a stable packing. Cylinders with different heights (H) and diameters (D), thus different shapes and aspect ratios (H/D), have been considered in six cases. In the first four cases, the cylinders are identical in each case, but have different height/diameter ratios, ranging from 0.025, 0.5, 5 to 50, with the corresponding shapes ranging from very thin disks to very long rods. In Case 5, two different types of cylinder are

(a) H/D = 0.025

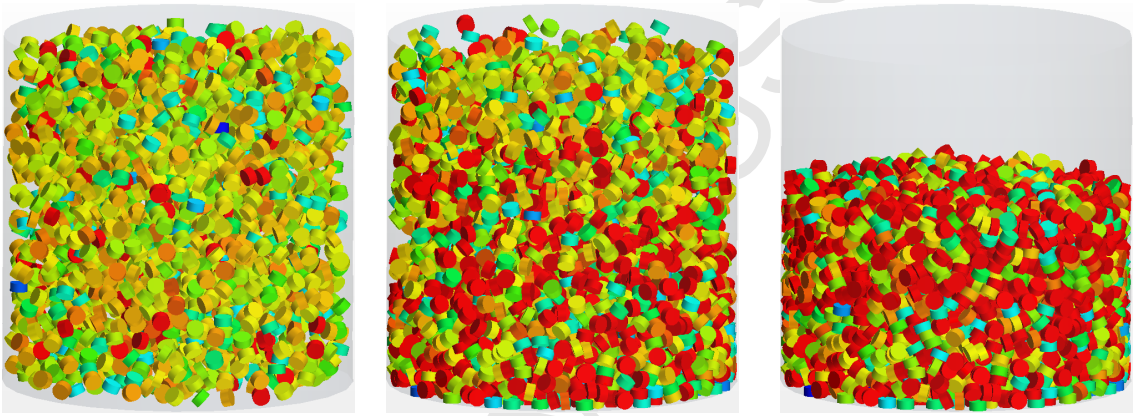

(b) H/D = 0.5

Figure 7: Packing configurations of cylinders at three stages with two different height (H)/diameter(D) ratios smaller than 1: (a) Case 1; (b) Case 2

mixed, one with H/D = 0.5 and the other H/D=10. In Case 6, both heights and diameters of cylinders obey a normal distribution, resulting in a wide variety of shapes and aspect ratios. The total number of cylindrical particles in each case is 5000.

The packing configurations at three stages (initial, middle and final) of the six cases are illustrated in Figures 7, 8 and 9 respectively. The colours in the figures are used to represent the orientations of particles but mainly for better visual effect. The axes of those cylinders with blue and green colours are more close to the vertical direction, while those with orange and red colours are closer to the horizontal directions.

The energy evolution of the particle systems during the packing is monitored. Both kinetic energy and total energy (potential + kinetic) for Case 5 are displayed in Figure 10, from which a two-phase process is evident. In the initial injection phase, both potential and kinetic energy increase when particles are continuously injected into the region until the total number of particles reaches the specified value. In the compaction phase, the total energy decreases as the kinetic energy is dissipated through damping during particle impact. A stable packing is achieved when the total kinetic energy reduces to zero and the total energy converges to the potential energy.

From the assessment point of view, the smaller the H/D ratio is, the more challenges to the proposed methodology will be presented, as more different contact configurations are encountered in the system. The fairly smooth nature of the kinetic energy evolution histories

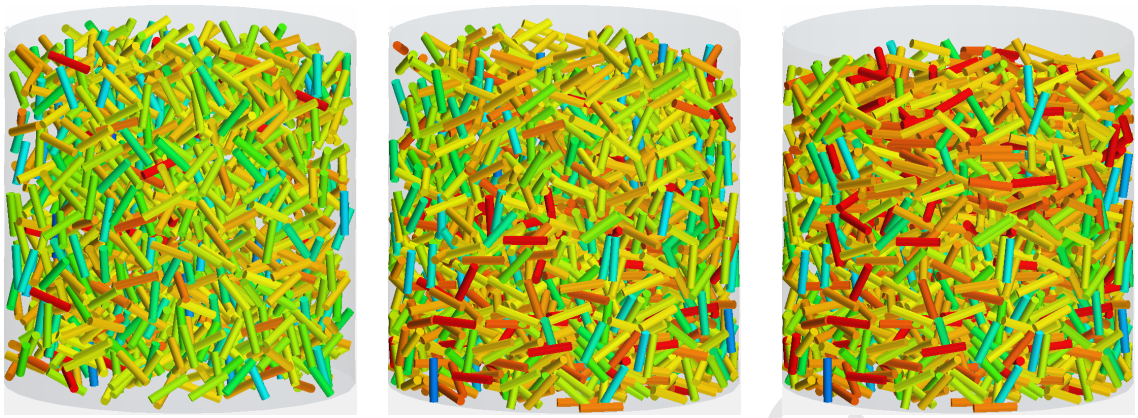

(a) H/D = 5

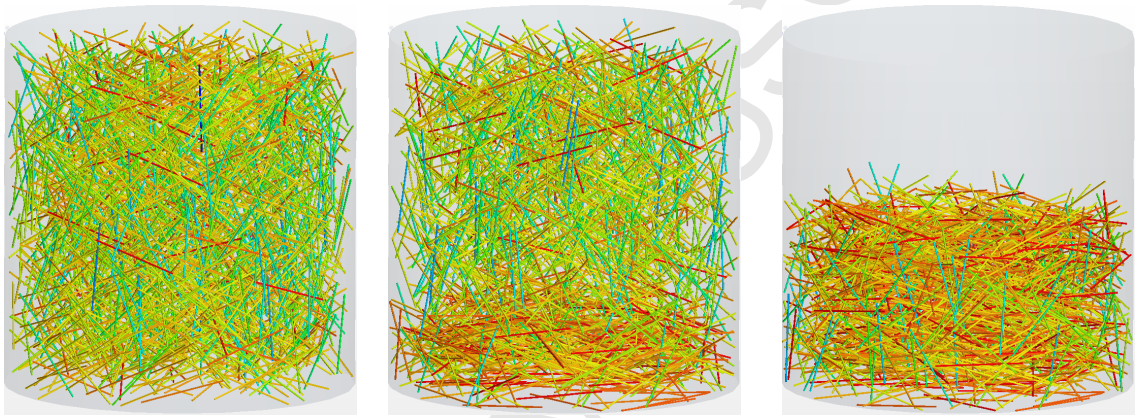

(b) H/D = 50

Figure 8: Packing configurations of cylinders at three stages with two different height (H)/diameter(D) ratios larger than 1: (a) Case 3; (b) Case 4

for all the cases demonstrates that the current implementation is generally stable and robust.

In addition to the robustness issue, the computational efficiency of the proposed methodology and its implementation is also an important consideration. A number of engineering applications have been employed to assess the performance of the method and implementation. In particular, cylindrical particle problems using the current cylinder model has been compared with the model using composite particles where each cylinder is approximately represented by a number of bonded/clumped spheres. The simulation shows [25] that for a transportation problem, the current cylindrical model is around 1.7 $\sim$ 2 times faster than the composite particle model using 20 spheres, thus indicating that for the given problem, the current cylinder-cylinder contact procedure is roughly about 10 times slower than a sphere-sphere contact detection.

As the physical modelling aspect of cylindrical particles is not covered in this work, no test results will be presented to demonstrate the physical correctness of the current model for cylindrical particle systems, such as conservation of energy during impact etc.

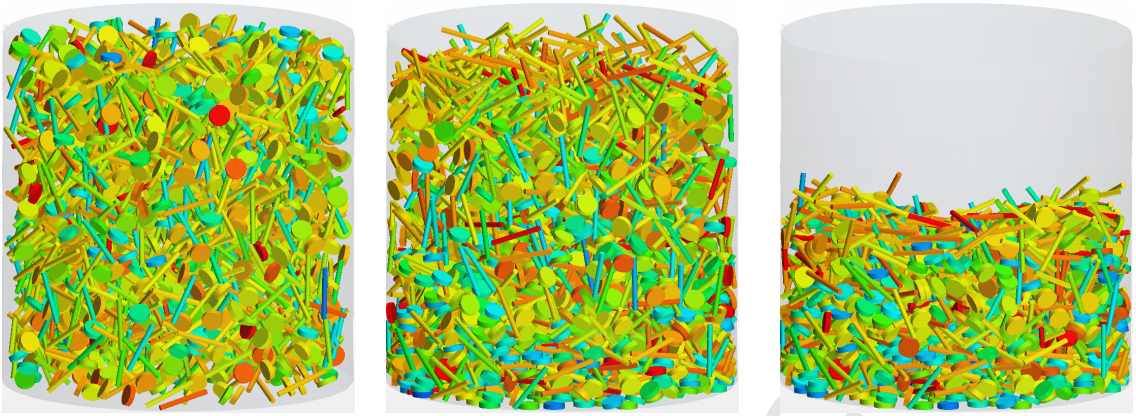

(a) Mixed cylinders with two height/daimeter ratios: 0.025 and 10

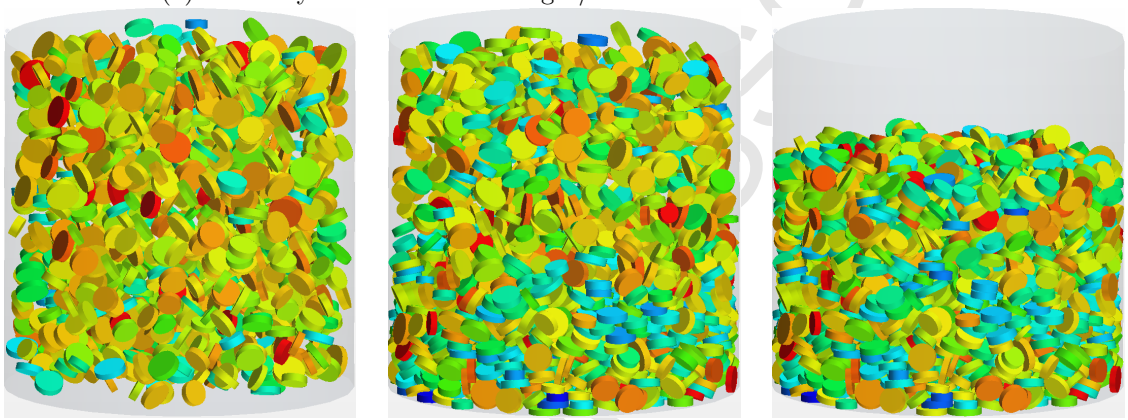

(b) Cylinders with normally distributed heights and radii

Figure 9: Packing configurations of cylinders at three stages with two different cylinder systems: (a) Case 5; (b) Case 6

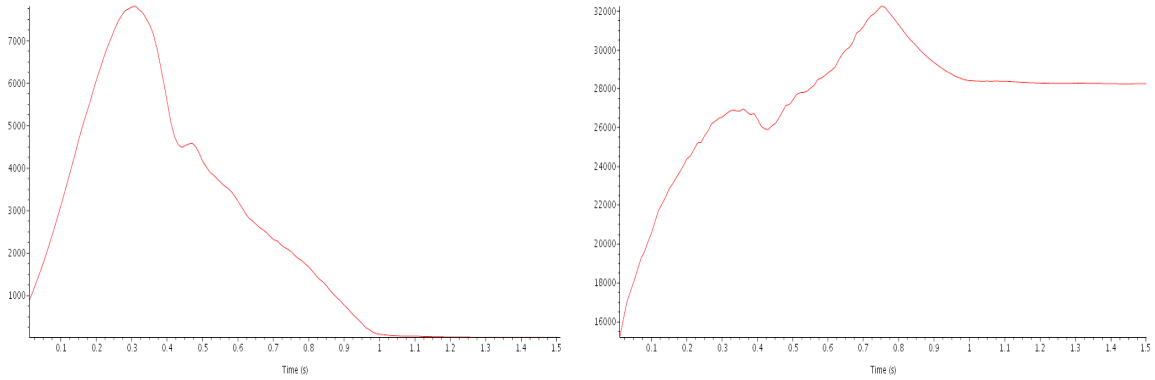

(a) Kinetic energy (b) Total energy

Figure 10: Evolution of kinetic and total energy for case 6

7 Concluding Remarks

By fully exploiting the axi-symmetry properties of a cylinder, a generic framework for detecting contact between cylindrical particles in discrete element modelling has been developed. The main contributions are:

- An effective 4-parameter local representative scheme is derived in a simple manner to

describe the spatial relationship between two cylinders so that the original 3D cylinder-cylinder intersection problem can be reduced to a serial of 2D circle-ellipse intersections, considerably simplifying the contact detection procedure;

- A two-stage contact detection scheme is proposed in which no-overlap contact pairs are identified with minimum computational costs in the first stage. The actual overlap region is determined and represented in the second stage. For the two overlap region representation schemes proposed, the layered region representation is generic, while the edge representation is more numerically efficient, but of an approximate nature. The proposed contact detection scheme imposes no limitations on (relative) sizes and aspect ratios of cylinders, and minimises the number of possible checks for different contact configurations, thereby resulting in a more generic and robust cylinder contact detection framework.

- The most significant contribution is the development of the two theorems that establish a fundamental relationship between the contact point and contact normal. These two theorems not only remove the ambiguity in determining the normal direction and/or provide a means to fine tune the contact point if necessary, but also guarantee that no superficial rotational energy is introduced into the system, making the numerical simulation more stable. They are therefore of both theoretical and practical significance.

It is important to highlight that all these developments are not only valid for cylinders but also can be extended to any axi-symmetrical shapes and their combinations with some modifications if necessary. The current work thus is a significant step towards effectively adopting cylinders, and potentially other axi-symmetrical geometric entities, as primitive discrete elements.

References

[1] P. A. Cundall, O. D. L. Strack. A discrete numerical model for granular assemblies. *Gotechnique* 29(1):47-65, 1979.

[2] J. M. Ting. A robust algorithm for ellipse-based discrete element modelling of granular materials. *Computers and Geotechnics* 13(3): 175-186, 1992.

[3] J. M. Ting, M. Khwaja, L. R. Meachum, J. D. Rowell. An ellipse-based discrete element model for granular materials. *Int. J. Numer. Anal. Meth. Geomech.*, 17: 603623, 1993.

[4] T.-T. Ng. Numerical simulations of granular soil using elliptical particles. *Computers and Geotechnics* 16(2): 153-169, 1994.

[5] J. R. Williams, A. Pentland. Superquadrics and model dynamics for discrete elements in interactive design. *Engineering Computations* 9:115128, 1992.

[6] X. Lin, T.-T. Ng. Contact detection algorithms for three-dimensional ellipsoids in discrete element modelling. *Int. J. Numer. Anal. Meth. Geomech.*, 19(9): 653659, 1995.

[7] X. Lin, T.-T. Ng. A three-dimensional discrete element model using arrays of ellipsoids. *Gotechnique* 47(2):319-329, 1997.

[8] M. A. Hopkins Discrete element modeling with dilated particles. *Engineering Computations* 21(2/3/4): 422 - 430, 2004.

[9] Y. T. Feng, D. R. J. Owen. A 2D polygon/polygon contact model: algorithmic aspects. *Engineering Computations.* 21: 265-277, 2004.

[10] P. A. Cundall. Formulation of a three-dimensional distinct element modelPart I. A scheme to detect and represent contacts in a system composed of many polyhedral blocks. *International Journal of Rock Mechanics and Mining Sciences and Geomechanics* 25:107116, 1988.

[11] Y. T. Feng, K. Han, D. R. J. Owen. An energy based polyhedron-to-polyhedron contact model. *Proceedings of 3rd M.I.T. Conference of Computational Fluid and Solid Mechanics*, MIT, USA, pp. 210214, 2005.

[12] K. Han, Y. T. Feng, D. R. J. Owen. Contact resolution for non-circular discrete objects. *Int. J. Numer. Meth. Engng.* 66(3):485-501, 2006.

[13] Y. T. Feng, K. Han, D. R. J. Owen. Energy-conserving contact interaction models for arbitrarily shaped discrete elements. *Comput. Methods Appl. Mech. Engrg.* 205-208: 169-177, 2012.

[14] W. Zhou, G. Ma, X. L. Chang, Y. Duan. Discrete modeling of rockfill materials considering the irregular shaped particles and their crushability. Engineering Computations 32(4): 1104 - 1120, 2015.

[15] K. L. Johnson. *Contact Mechanics.* Cambridge University Press, 1985.

[16] M. Kodam, R. Bharadwaj, J. Curtis, B. Hancock, C. Wassgren. Cylindrical object contact detection for use in discrete element method simulations: part I - Contact detection algorithms. *Chemical Engineering Science* 65(22): 5852-5862, 2010.

[17] M. Kodam, R. Bharadwaj, J. Curtis, B. Hancock, C. Wassgren. Cylindrical object contact detection for use in discrete element method simulations: part II - Experimental validation. *Chemical Engineering Science* 65(22): 5863-5871, 2010.

[18] Y. Guo, C. Wassgren, W. Ketterhagen, B. Hancock, J. Curtis. Some computational considerations associated with discrete element modeling of cylindrical particles. *Powder Technology* 228: 193-198, 2012.

[19] R. G. Chittawadigi, S. K. Saha. An analytical method to detect collision between cylinders using dual number algebra *Proceedings of the IEEE/RSJ International Conference on Intelligent Robots and Systems.* January 2013.

[20] J. D. Foley. *Computer graphics: principles and practice.* Addison-Wesley Professional, 1996. p. 113.

[21] W. H. Press, B. P. Flannery, S. A. Teukolsky, W. T. Vetterling. *Numerical Recipes in FORTRAN: The Art of Scientific Computing.* 2nd ed. Cambridge, England: Cambridge University Press, pp. 277 and 283-284, 1989.

[22] Y. T. Feng, K. Han, D. R. J. Owen. Filling domains with disks: An advancing front approach. *International Journal For Numerical Methods in Engineering.* 56: 699-713, 2003.

[23] K. Han, Y. T. Feng, D. R. J. Owen. Sphere Packing With a Geometric Based Compression Algorithm. *Powder Technology*, 155(1):33-41, 2005.

[24] USER GUIDE, STAR-CCM+ Version 11.02, CD-adapco, April, 2016.

[25] http://www.cd-adapco.com/node/8798 (last accessed: 07/04/2016)

Appendix 1. Find a closest point on an ellipse to the origin

This can be stated as the minimum problem:

$$f_{min} = \min_{x,y}\{f = x^2 + y^2\},\ \text{s. t. } \frac{(x-x_0)^2}{a^2} + \frac{(x-y_0)^2}{b^2} = 1 \tag{26}$$

where a and b are the two radii of the ellipse and (x_0, y_0) are its central coordinates.

Introduce the parametric equation of the ellipse in terms of θ:

$$x(\theta) = x_0 + a\cos\theta; \quad y(\theta) = y_0 + b\sin\theta$$

The first derivative of function f can be obtained as:

$$F(\theta) = \frac{df}{d\theta} = -ax\sin\theta + by\cos\theta \tag{27}$$

The minimum of f is found when $F(\theta) = 0$.

In the Newton-Raphson method, started with a given initial θ_0, θ is iteratively updated by

$$\theta_{i+1} = \theta_i - F(\theta_i)/F'(\theta_i)(i = 0, 1, ...)$$

where

$$F'(\theta) = \frac{F(\theta)}{d\theta} = a^2\sin^2\theta + b^2\cos\theta - ax\cos\theta - by\sin\theta$$

until the approximation solutions are determined when a pre-defined tolerance convergent criterion is satisfied.

Alternatively, $F(\theta) = 0$ can be cast as a quartic equation. Further set

$$x' = (x - x_0)/a;\ y' = (y - y0)/b,\ \text{thus } x'^2 + y'^2 = 1$$

then

$$F(\theta) = -ax\sin\theta + by\cos\theta = -axx' + byy'$$

$F(\theta) = 0$ gives

$$axx' = byy'$$

Substituting x by x' and y by y', and further eliminating y' leads to the following quartic equation in terms of x':

$$a_4x'^4 + a_3x'^3 + a_2x'^2 + a_1x' + a_0 = 0$$

where $a_4 = \alpha^2 - \beta^2; a_3 = 2\alpha\beta; a_2 = \beta^2 + \gamma^2 - \alpha^2; a_1 = -a_3, a_0 = -\beta^2$; and $\alpha = a^2 - b^2; \beta = ax_0$; and $\gamma = by_0$. To obtain a similar equation in terms of y', simply swap a and b, and x_0 and y_0.

Appendix 2. Intersections between a circle and an ellipse

Assume that the circle has a radius of r and its centre at the origin of the coordinate system, and that the ellipse has two radii of a and b, and its centre is located at (x_0, y_0). The intersection points of the two curves satisfy the equations

$$x^2 + y^2 = 1; \quad \text{and} \quad \frac{(x-x_0)^2}{a^2} + \frac{(y-y_0)^2}{b^2} = 1 \tag{28}$$

Eliminating y from the above two equations leads to the following quartic equation:

$$a_4x^4 + a_3x^3 + +a_2x^2 + +a_1x + a_0 = 0$$

where $a_4 = \alpha^2; a_3 = 2\alpha\beta; a_2 = \beta^2 + 2\alpha\gamma + \tau^2; a_1 = 2\beta\gamma, a_0 = r^2(1-\tau^2)$. Again, to obtain a similar equation in terms of y, simply swap a and b, and x_0 and y_0.

Appendix 3. Proofs of Contact Normal and Contact Point Theorems

I. Proof of Contact Normal Theorem

First to prove that the second part of the formula (23) is true.

Consider the normal direction line which passes through the contact point $\mathbf{p}$, and intersects both axes of the two cylinders as required. Assume that $\mathbf{q}$ is the intersection point on $\mathbf{n}_2$. The position of $\mathbf{q}$ can be expressed in terms of a parameter t:

$$\mathbf{q}(t) = \mathbf{c}_2 + t\ \mathbf{n}_2 \tag{29}$$

Let $\mathbf{n}_p$ be the normal to the plane π formed by the contact point $\mathbf{p}$ and the axis $\mathbf{n}_1$ (through $\mathbf{c}_1$):

$$\mathbf{n}_p = (\mathbf{p} - \mathbf{c}_1) \times \mathbf{n}_1 \tag{30}$$

By the definition, the line $\vec{pq}$ must lie on the plane π, and thus is perpendicular to the normal of the plane $\mathbf{n}_p$:

$$(\mathbf{q} - \mathbf{p}) \cdot \mathbf{n}_p = 0 \tag{31}$$

i.e.

$$(\mathbf{c}_2 - \mathbf{p} + t\ \mathbf{n}_2) \cdot \mathbf{n}_p = 0 \tag{32}$$

which gives

$$t = \frac{(\mathbf{c}_2 - \mathbf{p}) \cdot \mathbf{n}_p}{\mathbf{n}_2 \cdot \mathbf{n}_p} \tag{33}$$

Then the line $\vec{pq}$ should be co-linear with the contact normal line and the normal direction $\mathbf{n}$ (not normalised) thus can be determined as

$$\mathbf{n} = \mathbf{q} - \mathbf{p} = \mathbf{c}_2 - \mathbf{p} + t\ \mathbf{n}_2 \tag{34}$$

which is the second part of the formula (23). The first part can be proved similarly.

II. Proof of Contact Point Theorem

First to prove that the formula (24) is true when $i = 2$.

Let $\mathbf{p}$ be the contact point whose position can be expressed in terms of two parameters t and λ:

$$\mathbf{p}(t, \lambda) = \mathbf{c}_2 + t\ \mathbf{n}_2 + \lambda\ \mathbf{n} \tag{35}$$

where $\mathbf{c}_2 + t\ \mathbf{n}_2$ defines the point $\mathbf{q}$ that is the intersection point between the contact normal line and the 2nd cylinder axis $\mathbf{n}_2$. Again define $\mathbf{n}_p$ to be the normal to the plane π formed by the contact point $\mathbf{p}$ and the first cylinder axis $\mathbf{n}_1$ (passing through $\mathbf{c}_1$)

$$\mathbf{n}_p = (\mathbf{c}_1 - \mathbf{p}) \times \mathbf{n}_1 \tag{36}$$

and use the same argument as in the previous theorem that the normal direction $\mathbf{n}$ must be perpendicular to the normal of the plane $\mathbf{n}_p$:

$$\mathbf{n} \cdot \mathbf{n}_p = 0 \tag{37}$$

Substituting Eq (35) into (36), and then into (37) yields:

$$\mathbf{n} \cdot [(\mathbf{c}_1 - \mathbf{c}_2 + t\ \mathbf{n}_2 + \lambda\ \mathbf{n}) \times \mathbf{n}_1 = 0 \tag{38}$$

Expanding the brackets and utilising the fact that $\mathbf{n} \cdot (\mathbf{n} \times \mathbf{n}_1) = 0$ leads to

$$t = \frac{\mathbf{n} \cdot [(\mathbf{c}_1 - \mathbf{c}_2) \times \mathbf{n}_1]}{\mathbf{n} \cdot (\mathbf{n}_2 \times \mathbf{n}_1)} \tag{39}$$

So now $\mathbf{p}$ can be defined by (24) and λ becomes a free parameter. Thus the formula (24) is proved to be true when $i = 2$. The $i = 1$ case can be proved similarly.

Appendix 4. The Lin-Bairstow method for solving a quartic equation

Let the quartic equation be

$$P_4(x) = a_4x^4 + a_3x^3 + a_2x^2 + a_1x + a_0 = 0$$

It is numerically more efficient if $a_4 = 1$, which can be achieved by dividing all the a_i by a_4. Given two parameters $\{u, v\}$, $P_4(x)$ can be rewritten as

$$P_4(x) = Q_2(x)(x^2 + ux + v) + R(x)$$

where $Q_2(x) \equiv b_2x^2 + b_1 + b_0$ is a quadratic quotient and $R(x) \equiv cx + d$ is a linear reminder, with

$$b_2 = a_4; b_1 = a_3 - ub_2; b_0 = a_2 - ub_1 - vb_2$$

and

$$c = a_1 - ub_0 - vb_1 \equiv c(u, v);\ d = a_0 - vb_0 \equiv d(u, v)$$

$Q_2(x)$ divides $P_4(x)$ when $R(x) = 0$, i.e.

$$c(u, v) = 0;\ d(u, v) = 0 \tag{40}$$

These two equations in terms of u and v can be solved simultaneously by Newton's method:

$$\begin{bmatrix} u \\ v \end{bmatrix} \leftarrow \begin{bmatrix} u \\ v \end{bmatrix} - \mathbf{J}^{-1} \begin{bmatrix} c \\ d \end{bmatrix} \tag{41}$$

where

$$\mathbf{J} = \begin{bmatrix} \frac{\partial c}{\partial u} & \frac{\partial d}{\partial v} \\ \frac{\partial c}{\partial v} & \frac{\partial d}{\partial v} \end{bmatrix};\quad \mathbf{J}^{-1} = \frac{1}{vg^2 + h(h - ug)} \begin{bmatrix} -h & g \\ -gv & gu - h \end{bmatrix}$$

in which $g = b_1 - ub_2; h = b_0 - vb_2$. When a set of solutions $\{u, v\}$ is found, the solutions to the original quartic equatation can be obtained as:

$$x_{1,2} = (-u \pm \sqrt{u^2 - 4v})/2;\ x_{3,4} = (-b_1 \pm \sqrt{b_1^2 - 4b_2b_0})/2b_2$$

in which the number of real solutions can be 0, 2 or 4.

The same procedure can be applied to solve a cubic equation by setting $a_4 = 0$, and thus $b_2 = 0, b_1 = a_3, b_0 = a_2 - ub_1, g = b_1$ and $h = b_0$.

Research Highlights:

- **Develops a generic framework for detecting contact between cylindrical particles in discrete element modelling based on a full exploitation of the axi-symmetrical property of cylinders.**
- **Derives a four-parameter based local representative system to describe the spatial relationship between two cylinders so that the 3D cylinder-cylinder intersection problem can be reduced to a series of 2D circle-ellipse intersections, which considerably simplifies the contact detection procedure.**
- **Proposes a two-stage contact detection scheme in which no-overlap contact pairs are identified in the first overlap check stage, and then the actual overlap region is determined in the second resolution stage and represented by two schemes: the layered representation which is generic, and the edge representation which is numerically more efficient but less accurate.**
- **Develops two theorems that establish a fundamental relationship between the contact point and contact normal of two contacting cylinders, offering a simple approach to determining the normal direction based on the contact point and vice versa.**
- **These theorems are valid not only for cylinders, but also for any axi-symmetrical shapes and their combinations.**